EIGHTH EUROPEAN ROTORCRAFT FORUM

Paper No 3.10

THE INFLUENCE OF DIFFERENT INFLOW MODELS ON THE COUPLED FLAPPING AND TORSION OF HELICOPTER ROTOR BLADES

A. ROSEN, Z. BEIGELMAN

HAIFA, ISRAEL

August 31 through September 3, 1982

AIX-EN-PROVENCE, FRANCE

ASSOCIATION AERONAUTIQUE ET ASTRONAUTIQUE DE FRANCE

The Influence of Different Inflow Models on the Coupled Flapping and Torsion of Helicopter Rotor Blades

by

A. Rosen and Z. Beigelman

Abstract

Recently a model to calculate the influence of elastic pitch variations on the tip path plane dynamics, has been developed. This is a simplified efficient model which is especially suited for stability and control problems of modern helicopters having rotors which are flexible in torsion. In the present paper this model is used in order to investigate the influence of center of mass and aerodynamic center cross sectional locations on the elastic pitch variations and tip path plane steady state and time response. The investigation also includes the comparison between five different models of the induced velocity distribution over the disc. It is shown that all these parameters have a significant influence on the tip path plane dynamics. These influences should be taken into account when stability and control problems of modern rotors are analysed.

1. Introduction

For a long time helicopter rotor blades were designed to be relatively stiff in torsion and therefore influences of elastic torsion were neglected in many cases. During recent years it has been shown by different investigations, of which [1-5] are representative examples, that significant torsional deformations may have beneficial effects concerning performance, vibrations, aeroelastic behavior and other aspects of helicopter flight. Therefore, it is expected that an increasing number of rotors will exhibit significant elastic torsional deformations during operation [6]. It is clear that in the case of such modern rotors the elastic pitch variations are important and should be taken into account. There are cases where a detailed structural analysis of these torsional effects, like a few of the analyses in the above mentioned references, is required. These cases include the areas of: aeroelastic stability, vibrations, loads distribution etc. On the other hand it seems that for other purposes, like stability and control problems of the whole vehicle, a simple model which takes into account the elastic pitch variations, is most suitable.

Recently such a model was developed and presented [7]. In [7] the derivation of the model and the assumptions behind the derivation were presented. As an example of the application of the model the modes and eigenvalues associated with the Tip Path Plane (T.P.P) dynamics were calculated. In addition, the influence of aerodynamic moment along the blade on the steady state behavior of the T.P.P. has also been presented. In this case the simple model of a uniform inflow over the disc was used. It is well

known that while the modes and eigenvalues are not influenced by the inflow model, this model may have an important influence on the steady state flapping of the rotor, or the time response of the rotor as a result of command inputs.

The purpose of the present paper is to present the influence of elastic pitch variations on the T.P.P. steady state and time response. Therefore, special emphasis is made on investigating the influence of using different inflow models. This influence will be added to the important influences that blade's cross sectional center of mass and aerodynamic center locations have on the elastic pitch variations and therefore, also on the T.P.P. dynamics.

For the sake of completeness a brief description of the analytical model which has been developed in [7] is presented at the beginning. Later five different models of induced velocity distribution will be presented. Then the influence of the cross sectional center of mass and aerodynamic center locations on the steady state T.P.P. dynamics in the case of uniform induced velocity, in hovering and fast forward flight, will be investigated. The results of the uniform model will be compared with the other nonuniform aerodynamic models. At last the influence of different aerodynamic models on the time response will be shown.

2. The Rotor Model

The derivation of the rotor model has been presented in [7] and a more detailed presentation may be found in [8]. In this section a brief description of the rotor model is brought. Only general details which are important to the completeness and clarity of the present paper are presented. The interested reader may find the rest of the details in [7, 8].

The system of coordinates which are used in the present study are shown in Fig. 1. The point O coincides with the center of the rotor hub. x_{HUB}, y_{HUB} and z_{HUB} are the hub system of coordinates which are fixed with respect to the helicopter fuselage while z_{HUB} coincides with the rotor shaft and x_{HUB} points towards the helicopter front. $\hat{x}_{HUB}$, $\hat{y}_{HUB}$ and $\hat{z}_{HUB}$ are unit vectors in the directions x_{HUB}, y_{HUB} and z_{HUB}, respectively. The rotor rotates with a constant angular velocity Ω. The azimuth angle of the blade at each moment is given by ψ (see Fig. 1). If $\bar{R}_{HUB}$ is the position vector of the hub with respect to an inertial system, then the translational velocity and acceleration are given by:

$$\dot{\bar{R}}_{HUB} = u_{HUB}\,\hat{x}_{HUB} + v_{HUB}\,\hat{y}_{HUB} + w_{HUB}\,\hat{z}_{HUB} \tag{1}$$

$$\ddot{\bar{R}}_{HUB} = a_{xHUB}\,\hat{x}_{HUB} + a_{yHUB}\,\hat{y}_{HUB} + a_{zHUB}\,\hat{z}_{HUB} \tag{2}$$

In addition, the hub system also exhibits a rotational velocity $\bar{Q}$ given by:

$$\bar{Q} = p\,\hat{x}_{HUB} + q\,\hat{y}_{HUB} + r\,\hat{z}_{HUB} \tag{3}$$

As usual it is assumed the p, q and r are small compared to Ω. In the analysis only flapping of the blade is considered. The flapping angle is denoted by β (see Fig. 1) and the derivation is restricted to the common cases where β is a small angle.

It is convenient to calculate the aerodynamic contributions using wind coordinates. Therefore, the fuselage fixed hub coordinates are replaced by the hub-wind coordinates x_{HUBW}, y_{HUBW}, z_{HUBW}, which are shown in Fig. 2. This hub-wind system is rotated relative to the hub system by the side slip angle β_w. A new azimith angle, ψ_w, is also defined as:

$$\psi_w = \psi + \beta_w \tag{4}$$

It should be noted that β_w is generally time dependent. The derivation will be restricted to the practical cases where $\dot{\beta}_w$ (a dot indicates differentiation with respect to time) is much smaller than Ω. In calculating the aerodynamic loads, the induced velocity plays a major roll. This velocity will be denoted by v_i and it acts in the direction $\hat{z}_{HUB}$. The model of induced velocity which will be used in the present analysis is presented by the following equation:

$$\lambda_i = v_i/\Omega R = \lambda_{io}\, f_{\lambda_{io}}(x) + \lambda_{ic}\, f_{\lambda_{ic}}(x)\cos\psi_w + \lambda_{is}\, f_{\lambda_{is}}(x)\sin\psi_w \tag{5}$$

where R is the radius of the rotor and x is a nondimensional spanwise coordinate which is obtained after dividing (e+r') (see Fig. 1) by R.

The pitch angle along the blade, θ, is given by:

$$\theta = \theta_o - A_{1c}\cos\psi_w - B_{1c}\sin\psi_w + (x-\varepsilon)(\theta_{tob} + \theta_{toe} - \theta_{tc}\cos\psi_w - \theta_{ts}\sin\psi_w) - K_1\beta \tag{6}$$

θ_o is the root collective pitch while A_{1c} and B_{1c} represent the root cyclic pitch. θ_{tob} is the linear built in twist while θ_{toe}, θ_{tc}, and θ_{ts} present elastic linear pitch variations along the blade. K_1 represents the coupling between flapping and pitch motions due to δ_3 or other elastic coupling effects. ε is a nondimensional offset which equals to e divided by R.

Except for the blade torsional flexibility, the flexibility of the control system is also taken into account. The stiffness and damping of the control system determine the relation between the pitch motion at the blade root and the pilot or augmentation system command, θ_p, which is given by:

$$\theta_p = \theta_{op} - A_{1p}\cos\psi_w - B_{1p}\sin\psi_w \tag{7}$$

Since a simplified model of the rotor which is appropriate for mechanics of flight and control applications is of interest here, the following well known expression for the flapping angle is used:

$$\beta(t) = a_0(t) - a_1(t)\cos\psi_w - b_1(t)\sin\psi_w \tag{8}$$

where higher harmonics are neglected.

The vector of unknowns becomes:

$$\{x_R\}^T = \langle a_0,\ a_1,\ b_1,\ \theta_0,\ A_{1c},\ B_{1c},\ \theta_{to},\ \theta_{tc},\ \theta_{ts} \rangle \tag{9}$$

where θ_{to} is the sum of θ_{tob} and θ_{toe}.

A tedious analytical derivation [7, 8] yields a linear differential system of nine coupled equations in the nine unknowns. This system is represented by the following equation:

$$[A1]\{\ddot{x}_R\} + [A2]\{\dot{x}_R\} + [A3]\{x_R\} = [A4]\{\lambda\} + [A5]\{q\} + \{A6\}tg\alpha + [A7]\{\dot{\theta}_p\} + [A8]\{\theta_p\} + \{A9\} \tag{10}$$

[A1], [A2] and [A3] are matrices of dimension (9x9). [A4], [A7] and [A8] are (9x3) matrices. [A5] is a (9x4) matrix while {A6} and {A9} are vectors of order 9. All the elements of these matrices and vectors are functions of the rotor aerodynamic, inertia and structural properties, the control system properties, and the flight conditions, and are defined in [7, 8]. The inflow vector is defined as:

$$\{\lambda\}^T = \langle \lambda_{io},\ \lambda_{ic},\ \lambda_{is} \rangle \tag{11}$$

The vector q equals:

$$\{q\}^T = \langle \tilde{p}_w,\ \tilde{q}_w,\ \dot{\tilde{p}}_w,\ \dot{\tilde{q}}_w \rangle \tag{12}$$

where

$$\tilde{q}_w = (q\cos\beta_w - p\sin\beta_w)/\Omega \tag{13a}$$

$$\tilde{p}_w = (q\sin\beta_w + p\cos\beta_w)/\Omega \tag{13b}$$

$$\dot{\tilde{q}}_w = (\dot{q}\cos\beta_w - \dot{p}\sin\beta_w)/\Omega^2 \tag{13c}$$

$$\dot{\tilde{p}}_w = (\dot{q}\sin\beta_w + \dot{p}\cos\beta_w)/\Omega^2 \tag{13d}$$

α is the angle of attack of the shaft (see Fig. 2) while $\{\theta_p\}$ is the command vector defined as:

$$\{\theta_p\}^T = <\theta_o, A_{1p}, B_{1p}> \tag{14}$$

3. The Induced Velocity Models

Five different models of the induced velocity have been used during the course of the present investigation. All these models fall within the general description of Eq. (5).

The simplest model, which is very popular and successful for many applications, is the uniform induced velocity, which has been suggested by Glauert [9]. According to this model

$$\lambda_i = \sqrt{\frac{-\mu^2 + \sqrt{\mu^4 + C_T^2}}{2}} \tag{15}$$

where μ is the advance ratio while C_T is the thrust coefficient. In order to use Eq. (15) during the present analysis, an expression for C_T as a function of the rotor properties is necessary. For this purpose the well known following equation is used (see for example [10])

$$C_T = \frac{\sigma a_{0.75}}{4}\left[\frac{2}{3}\theta_{0.75}(1 + \frac{3}{2}\mu^2) + \mu tg\alpha - \lambda_i - \mu B_{1c}\right] \tag{16}$$

where σ is the rotor solidity while $a_{0.75}$ and $\theta_{0.75}$ are the lift coefficient curve slope and collective pitch angle at the representative 0.75 span cross section. The validity of the last equation has been shown by many investigators. Substitution of Eq. (16) into Eq. (15) leads to an algebric fourth order equation in λ_i where the real positive root is the only result of physical meaning. It should be noted that $\theta_{0.75}$ includes the influence of the elastic pitch variation θ_{toe}. Since θ_{toe} is a function of the aerodynamic loads which are functions of λ_i, iterative procedure should be used in order to solve the problem.

Glauert himself felt that the uniform model is only a first order approximation and suggested a more complicated model where the induced velocity is varied linearly along the disc. A similar model which was derived by Coleman et al. [11], and is also described in [12], will be the second model. According to this model:

$$\lambda_i = \lambda_{io}(1 + K_x x \cos\psi) \tag{17}$$

λ_{io} is identical with the uniform value of λ_i as obtained from the first model. K_x is defined by the following equation:

$$K_x = tg\chi/2 \tag{18}$$

where χ is the wake skew angle which is given by:

$$tg\chi = \mu/(\lambda_{io} - \mu tg\alpha_D) \tag{19}$$

α_D is the disc angle of attack which equals:

$$\alpha_D = \alpha + a_1 \tag{20}$$

Since α_D is a function of a_1 which is an element in the vector of unknowns, it is clear that the solution will require an iterative procedure.

Drees [13] suggested a more complicated model which is the third model of the present investigation. According to this model:

$$\lambda_i = \lambda_{io}(1 + K_x \times \cos\psi + K_y \times \sin\psi) \tag{21}$$

where

$$K_x = \frac{4}{3}\frac{1-\cos\chi - 1.8\mu^2}{\sin\chi} \tag{22a}$$

$$K_y = -2\mu \tag{22b}$$

The fourth model is a result of a derivation by Mangler and Squire [14]. This model was obtained by solving the flow field through the disc. Their results were presented as an infinite Fourier series. Taking only the first harmonic, the following result is obtained:

$$\lambda_i = 4\lambda_{io}(\frac{1}{2} C_o + C_1 \cos\psi) \tag{23a}$$

$$C_o = \frac{15}{8}\sqrt{1 - x^2}\, x^2 \tag{23b}$$

$$C_1 = \frac{15\pi}{256}(4 - 9x^2) \times \sqrt{\frac{1-\sin\alpha_D}{1+\sin\alpha_D}}\, \sin\chi \tag{23c}$$

Equations (23a-c) represent load distribution III of [14]. The original results of Mangler and Squire were obtained for the case of relatively fast forward speed. Equations (22a-c) include an intuitive extension of the original results to also include low speeds and hover. This extension is presented by λ_{io} in Eq. (23a) and $\sin\chi$ in Eq. (23c).

The fifth and last model is according to White and Blake [15] who introduced their model in order to investigate the gust response of a rotor. This model was obtained after replacing the rotor and its complicated wake by a classical horseshoe vortex system which is very common in fixed-wing aerodynamics. λ_i is given by:

$$\lambda_i = \lambda_{io}(1 + \sqrt{2}\, x \sin\chi \cos\psi) \tag{24}$$

4. Results and Discussion

4.1 General

The theory which has been presented will be used in order to investigate the influence of elastic pitch variations on the T.P.P. dynamics of the rotor. As already mentioned special emphasis will be devoted to examining the influence of different induced velocity distribution models.

The numerical calculations are for Rotor II whose detailed properties are given in [7]. The rotor properties were chosen similar to the typical properties of the ATRS (Advanced Technology Rotor System) as described in [16], except for a smaller torsional rigidity which yield a first torsional frequency which is close to 4/rev. The rotor has four blades and except for a linear washout all the structural, mass and aerodynamic properties are considered uniform along the blades. The shaft angle of attack, α, is equal to zero in hover, and -5° in forward flight.

4.2 The Steady State Solution - Uniform Inflow

The steady state solution is obtained from Eq. (10) when $\{\ddot{x}_R\}$ and $\{\dot{x}_R\}$ are taken equal to zero. In [7] the influence of the aerodynamic moment on the steady state has been investigated and presented. Therefore in the present paper only the influences of the cross sectional aerodynamic center and center of mass locations on the behavior are described.

In Figs. 3a,b the influence of moving the aerodynamic center towards the leading and trailing edges, relative to the elastic axis, is presented. In this case the center of mass coincides with the elastic axis. The shift in the aerodynamic center is given in percents of a chord. In the figures the nondimensional values of the steady state flapping coefficients are presented (the wiggle above the variables indicate nondimensionality). In addition also the nondimensional elastic pitch components $\tilde{\theta}_{toe}$, $\tilde{\theta}_{tc}$, $\tilde{\theta}_{ts}$ are presented. The nondimensional terms are obtained after dividing the dimensional terms by the input collective pitch at 75% blade span. It should be point out that only a collective pitch command of 13.2° at the blade root is considered here, while A_{1p} and A_{1p} are taken equal to zero.

Figure 3a presents the axisymmetric case of hovering. Moving the aerodynamic center in front of the elastic axis results in a nose up moment along the blade. This moment result in an increase in $\tilde{\theta}_{toe}$ which in return results in an increase in the coning $\tilde{a}_0$.

A more complicated behaviour is presented in the asymmetric forward flight ($\mu = 0.3$) as shown by Fig. 3b. Again, as in hovering, moving the aerodynamic center towards the leading edge results in an increase in $\tilde{\theta}_{toe}$ which results in an increase of $\tilde{a}_0$. But in forward flight the increase in $\tilde{\theta}_{toe}$ also causes an increase in the disc blow back-meaning an increase in $\tilde{a}_1$. In addition, in the case of forward flight, an increase in $\tilde{a}_0$ results in an increase in the sideward tilt of the T.P.P., $\tilde{b}_1$. The periodic aerodynamic loads also cause periodic one per rev. linear elastic

pitch variations $\tilde{\theta}_{ts}$ and $\tilde{\theta}_{tc}$. The variations in the aerodynamic loads between the advancing and regressing blades are larger than the variations between the blades at the rearward and forward azimulthal locations. Therefore the magnitude of $\tilde{\theta}_{ts}$ is larger than $\tilde{\theta}_{tc}$. It should be noted that for negative values of y_{ac} the pitch angle is decreased on the advancing blade and increased on the regressing blade. This behavior results from the fact that there is an unloading of the tip of the advancing blade. This cyclic variation, $\tilde{\theta}_{ts}$, tends to decrease $\tilde{a}_1$. But for cases where the aerodynamic center is moved more than two percent of a chord towards the leading edge this tendency is smaller than the influence of $\tilde{\theta}_{toe}$ which has been mentioned and therefore $\tilde{a}_1$ is increased.

In the case of positive values of $y_{a.c.}$, $\tilde{\theta}_{toe}$ becomes negative and therefore the influence of the nonperiodic component of the pitch-which includes the collective pitch at the blade root, the built in twist and steady linear elastic pitch variation - is decreased considerably. On the other hand, in this case the pitch angle on the advancing blade is increased while the pitch angle of the retreating blade is decreased. This behavior results in a blow-back of the disc. Since the influence of the steady pitch is decreased the influence of the elastic cyclic pitch variations, unlike cases of $y_{a.c.} < -2\%$, becomes the dominant phenomenon. This change in the behavior of $\tilde{a}_1$ and $\tilde{b}_1$ is clearly seen in Fig. 3b. In this case $\tilde{\theta}_{tc}$ also contributes to the increase in $\tilde{b}_1$ unlike the case of negative values of $y_{a.c.}$.

Figures (4a, b) exhibit the influence of a shift in the cross sectional center of mass location relative to the elastic axis. In this case the aerodynamic center coincides with the elastic axis. Figure 4a presents the case of hovering. When the center of mass is shifted in front of the elastic axis, the centrifugal forces when coupled with the coning, result in a nose down torsional moment along the blade. This moment causes a decrease in the pitch angle which in return results in a decrease in the coning. The opposite situation occurs when the center of mass is shifted behind the elastic axis. It should be noted, as already has been indicated in [7, 8], that the case of the center of mass behind the elastic axis and aerodynamic center, is very dangerous and deserves special caution because of the possibility of a dangerous flapping-torsion flutter. The present analysis which only deals with the one per rev. T.P.P. motions is not capable of detecting this flutter phenomenon. The case of forward flight is described in Fig. 4b. The behavior of $\tilde{\theta}_{toe}$ and $\tilde{a}_0$ is similar to the case hover. In addition, because of the asymmetry of forward flight, a decrease in the collective pitch results in a smaller blow-back of the disc. As expected a decrease in $\tilde{a}_0$ also results in a decrease of $\tilde{b}_1$. The opposite trends appear while $\tilde{\theta}_{toe}$ increases as a result of moving the center of mass location behind the elastic axis.

4.3 The Influence of Different Induced Velocity Models on the Steady State Response.

In the previous subsection the steady response in the case of uniform induced velocity has been investigated and discussed. In the present subsection the influence of the four other nonuniform induced velocity models which were described in Section 3 - is presented. Figure 5 presents a comparison between the theoretical results of the different aerodynamic models and the experimental results of Harris [17]. Harris' results have already become one of the classics of helicopter experimental work and many investigators have presented comparisons of different theoretical predictions with these experimental results. Such a comparison is repeated in Fig. 5 in order to indicate the differences between the different theories and their agreement with experiments.

In the case of coning the experimental results exhibited a nominal angle of 3° throughout the whole speed range. The results of all the theories, except Mangler and Squire, are practically identical and show fairly good agreement with the experiments. The results according to Mangler and Squire are smaller and do not agree well with the experimental results at low advance ratios. The blow-back a_1 shows fairly good agreement between the experimental results and theoretical predictions. The deviations increase as the advance ratio is increased. In this case the results according to Mangler and Squire exhibit the best agreement with the experimental results. The most interesting case is that of the sideward tilt of the disc, b_1. At the region $0 < \mu < 0.2$ the results of using uniform induced velocity show very poor agreement with the experimental results. The other theories show much better agreement while the results according to White and Blake exhibit the best agreement with the experimental results in the problematic region of low advance ratios.

In the comparisons between the experimental results of Harris and the different induced velocity models, the blades were considered as rigid in torsion. In Figs. 6a-d the influence of different induced velocity models on the steady state flapping of the present rotor is investigated. The flapping coefficients are given as a function of the advance ratio throughout the region $0 \leq \mu \leq 0.4$.

Figure 6a presents the case where the aerodynamic center and center of mass locations coincide with the elastic axis. The coning a_0 is identical for all theories except for small values of μ where the results of Mangler and Squire are smaller. The blow-back, a_1, shows considerable differences at low advance ratios. The relative discrepancies decrease as μ is increased. As expected from the previous discussion of Fig. 5, very large discrepancies exist in the disc sideward tilt b_1, especially in the neighborhood of $\mu = 0.08$. These discrepancies decrease as μ is increased.

Figure 6b presents the case where the aerodynamic center is shifted two percent of a chord behind the elastic axis. As already explained in the discussion of Figs. 3a, b, in this case θ_{toe} is negative and the collective pitch at each cross section is decreased. As a result a small decrease in a_0 compared to Fig. 6a is obtained. As also explained in the previous

discussion the cyclic aerodynamic loads result in increasing negative values of e_{ts}. These cyclic elastic linear pitch variations result in an increase in a_1 compared to Fig. 6a. Concerning the comparison between the different aerodynamic models, trends which have been pointed out previously continue to appear and they will not be discussed again. It should be pointed out that the discrepancy in the results for a_1 at low advance ratios according to different models are increased due to the elastic pitch variations. Of special interest are the results of using the induced velocity distributions according to Drees [13]. This is the only model (among those which are considered here) where the sine component of the induced velocity is not zero. Such a component is equivalent to a cyclic pitch where, according to the present model, the pitch angle of the advancing blade is increased while the pitch angle of the regressing blade is decreased. As shown in Fig. 6a this "equivalent cyclic pitch" has a very small effect when elastic pitch variations are not presented. As shown by Fig. 6b this effect becomes important when elastic pitch variations, as a result of a rearward shift of the aerodynamic center, are introduced. In this case the periodic aerodynamic forces tend to decrease the pitch of the advancing blade and increase the pitch of the regressing one. This phenomenon results in a decrease in a_1. This decrease in the disc blow-back is also the reason for the small decrease in the coning a_0. The behavior of b_1 is similar to what has been indicated in the previous cases.

The case where the aerodynamic center is moved three percent of a chord in front of the elastic center is shown in Fig. 6c. As explained in Figs. 3a,b, in this case a large increase in e_{toe} is obtained which dominates the phenomenon. This increase in e_{toe} results in a significant increase in a_0 which in turn results in an increase in b_1. In addition, the increase in e_{toe} also results in an increase in the disc blow-back a_1, compared to Fig. 6a. It is interesting to note that usually the deviations between the results of the different induced velocity models at low advance ratio are decreased compared to Fig. 6a. Of special interest again is the model of Drees. In the present case of a forward shift of the aerodynamic center the sine component of the induced velocity causes a nose up moment on the advancing blade. Therefore an elastic linear cyclic pitch is caused where the pitch of the advancing blade is increased. This cyclic pitch results in an increase in a_1 which in turn causes higher induced velocities and therefore enhances the phenomenon. This diverging nature is easily recognized in Fig. 6c. The influence of the increase in a_1 on the coning a_0 is also shown very clearly. As in the previous cases the sensitivity of the sideward tilt to the different induced velocity models and to the behavior of a_0 and a_1 is also evident here.

The case where the center of mass is shifted two percent of a chord in front of the elastic axis (the aerodynamic center conincides with the elastic axis) is shown in Fig. 6d. As explained in Figs. 4a,b e_{toe} is decreased and this fact results in a decrease in a_0, a_1 and b_1 compared to Fig. 6a.

In the case of a center of mass shift, the elastic pitch variations are influenced by inertia contributions only. Therefore, unlike the case of a shift in the cross sectional aerodynamic center location, the differences between the different induced velocity models are very similar to those of Fig. 6a.

4.4 Time Response Simulation

In this kind of analysis it is assumed that the rotor is operating in a wind tunnel where μ and α are fixed during the experiment. Initially the rotor is operating at a certain steady state and at a time t=0, $\{\theta_p\}$ is changed in a known manner. The response of the rotor until it reaches a new steady state (when the phenomenon is stable) is calculated by integration of Eq. (10).

Figure 7 presents the time response of the present rotor while $\alpha=-5^\circ$, $\mu=0.3$, $y_{cg} = -2\%$, $y_{a.c.} = 0$. Initially the collective pitch at the root equals 8.9° and at the time t=0 a collective step input of $\theta_{op}=4.3^\circ$ is added. As indicated in the figure the results for uniform induced velocity distribution and the model of White and Blake [15], are presented. It is shown that the response of a_0 is identical in both cases while only very small deviations in the behavior of a_1 appear. In the case of b_1, as expected, large differences in the initial and final steady state values exist. Therefore, the time response between those two steady states is different. On the other hand the nature of the b_1 variation with time is identical in both cases.

Figure 8 exhibits the time response for the case $\alpha=-5^\circ$, $\mu=0.3$, $y_{cg}=0$, $y_{ac}=-2\%$. The initial conditions and input are the same as in the previous case. In this case the uniform induced velocity model is compared with the model of Drees. As expected from the results of the previous subsection, the initial and final flapping coefficients are different because of the different aerodynamic models. But the nature of the transient from the initial to the final steady states is identical in both cases and also identical to what has been shown in Fig. 7.

From Figs. 7, 8 it is also evident that practically the rotor reaches the new steady state during the time required for one revolution (the period in this case is 0.206 sec).

5. Conclusions

The cross sectional locations of the aerodynamic center and center of mass have a significant influence on the elastic pitch variations of the blades and therefore on the T.P.P. dynamics. A simplified rotor model which is suitable for helicopter stability and control problems is very efficient in calculating those influences. From the numerical results it is clear that for modern rotors which exhibit significant elastic pitch variations those variations should be taken into account when analysing problems of stability, control and performance of helicopters.

The aerodynamic model of induced velocity distribution over the disc is important and has an important influence on the results in many cases. As it is known for a long time the longitudinal variation of the induced velocity is very important because of its influence on the sideward tilt of the disc. In the case of elastic pitch variations the lateral induced velocity distribution becomes very important because of its influence on the blow-back of the disc.

Acknowledgements

The authors would like to thank Mrs. A. Goodman-Pinto for typing the paper and Mrs. R. Pavlic and Mrs. E. Nitzan for the preparation of the Figures.

List of References

1. R. Gabel and F. Tarzanin, Blade torsional tuning to manage large amplitude control loads, Journal of Aircraft, Vol. 11, No. 8, 1979 pp. 460-466.

2. G.S. Doman, F.J. Tarzanin and J. Shaw, Investigation of aeroelastically adaptive rotors, USAAMRDL TR-77-3, May 1977.

3. R.H. Blackwell and D.J. Merkley, The aeroelastically conformable rotor concept, Journal of the American Helicopter Society, Vol. 24, No. 4, 1979, pp. 37-44.

4. R.H. Blackwell, R.J. Murrell, W.T. Yeager and P.H. Mirick, Wind tunnel evaluation of aeroelastically conformable rotors, presented at the 36th Annual forum of the American Helicopter Society, Washington, D.C., May 1980. Also: Journal of American Helicopter Society, Vol. 26, No. 2, 1981, pp. 31-39.

5. J.G. Yen and W.H. Weller, Analysis and application of compliant rotor technology, presented at the 6th European Rotorcraft and Powered Lift Aircraft Forum, Bristol, England, Sept. 16-19, 1980.

6. D.P. Scharge and J.A. O'Malley, Performance and aeroelastic tradeoffs on recent rotor blade designs, Proceedings of the National Specialists' Meeting "Rotor System Design" Philadelphia, Penn., Oct. 1980.

7. A. Rosen and Z. Beigelman, A simplified model of the influence of elastic pitch variations on the rotor flapping dynamics, Proceedings of the 24th Israel Annual Conference on Aviation and Astronautics, 17-18 Feb., 1982, pp. 225-240.

8. A. Rosen and Z. Beigelman, A simplified model of the influence of elastic pitch variations on helicopter rotor flapping dynamics, TAE Report No. 480, Dept. of Aeronautical Engineering, Technion-Israel Institute of Technology, Haifa, Israel, March 1982.

9. H. Glauert, A general theory of the autogyro, ARC R and M 1111, Nov. 1926.

10. A.R.S. Bramwell, Helicopter dynamics, John Wiley and Sons, New York, 1976.

11. R.P. Coleman, A.M. Feingold and C.W. Stempin, Evaluation of the induced-velocity field of an idealized helicopter rotor, NACA ARR L5E10, June 1945.

12. W. Johnson, Helicopter theory, Princeton University Press, 1980.

13. J.M. Drees, A theory of airflow through rotors and its application to some helicopter problems, Journal of the Helicopter Association of Great Britain, Vol. 3, No. 2, July-Sept. 1949.

14. K.W. Mangler and H.B. Squire, The induced velocity field of a rotor, ARC R and M 2642, May 1950.

15. F. White and B.B. Blake, Improved method of predicting helicopter control response and gust sensitivity, Proceedings of the 35th American Helicopter Society Annual Forum, Paper No. 25, May 1979.

16. D. Jepson, R. Moffitt, K. Hilzinger and J. Bissell, Analysis and correlation of test data from an advanced technology rotor system, NASA CR-152336, July 1980.

17. F.D. Harris, Articulated rotor blade flapping motion at low advance ratio, Journal of the American Helicopter Society, Vol. 17, No. 1, 1972, pp. 41-48.

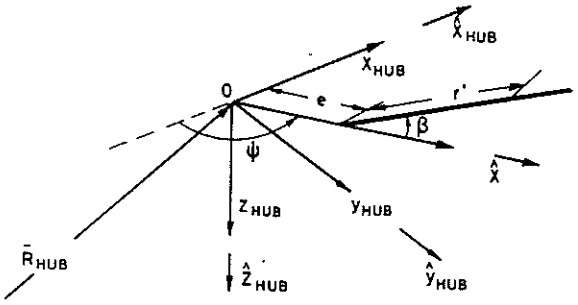

Fig. 1. System of Coordinates

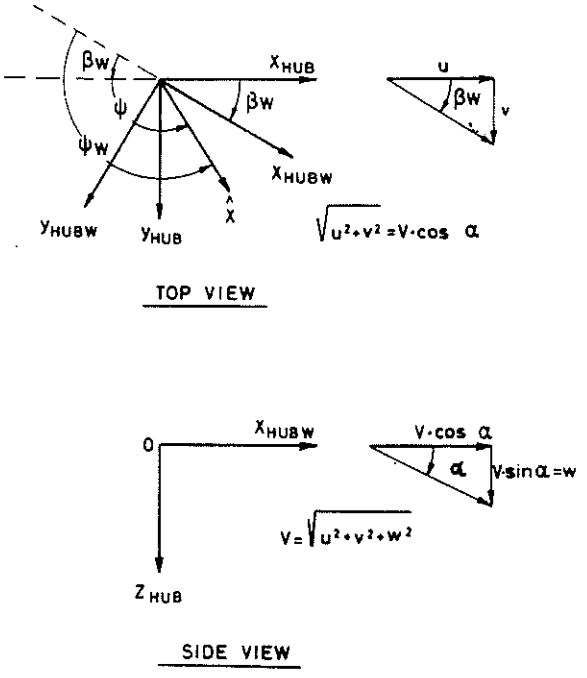

Fig. 2. Description of the Hub and Hub–Wind Systems of Coordinates.

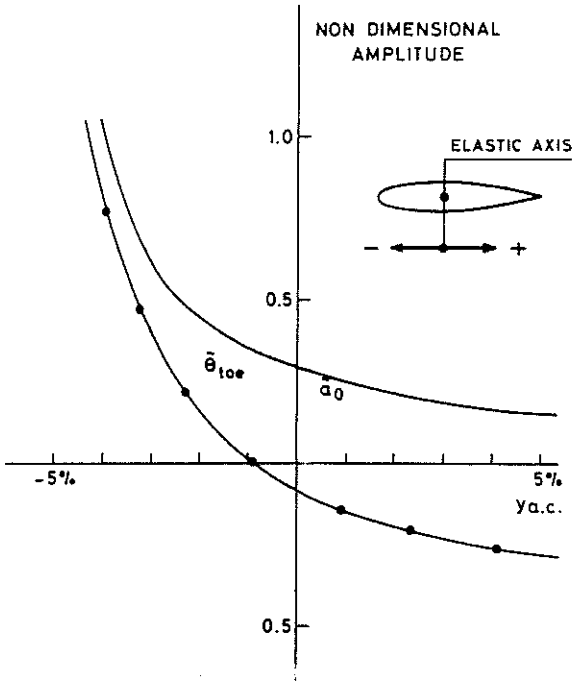

Fig. 3a. The Influence of Cross Sectional Aerodynamic Center Location on the Steady State Flapping and Elastic Pitch in Hover.

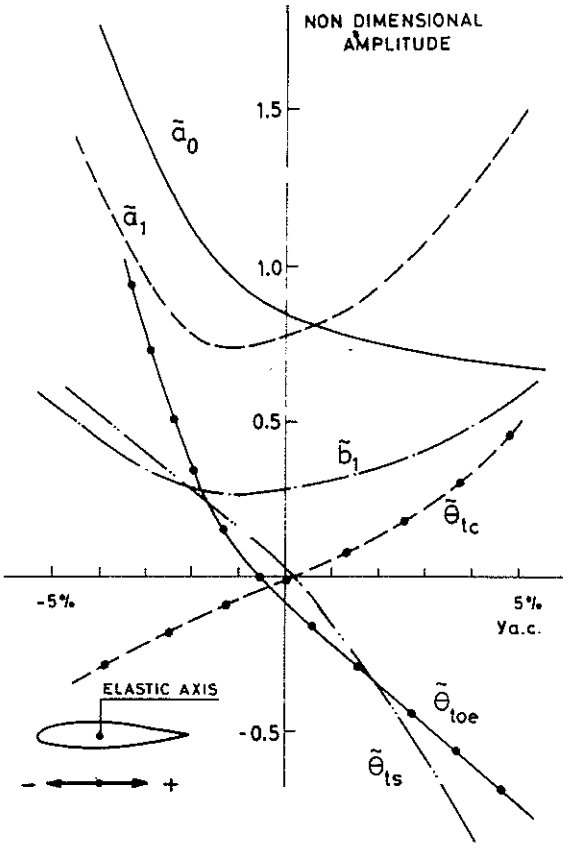

Fig. 3b. The Influence of Cross Sectional Aerodynamic Center Location on the Steady State Flapping and Elastic Pitch in Forward Flight (μ=0.3).

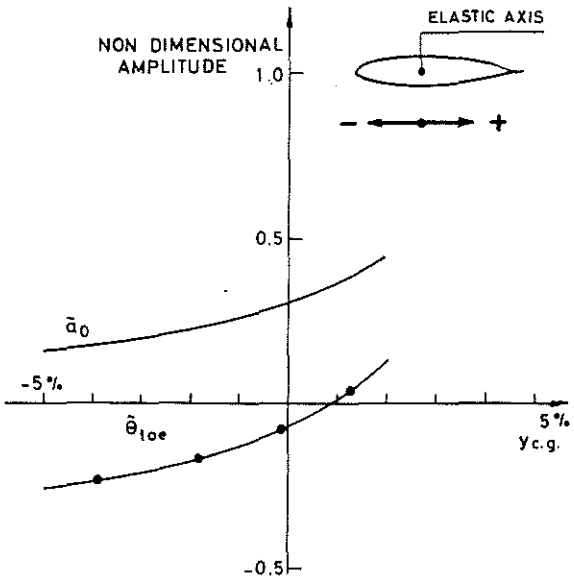

Fig. 4a. The Influence of Cross Sectional Center of Mass Location on the Steady State Flapping and Elastic Pitch in Hover - Rotor II.

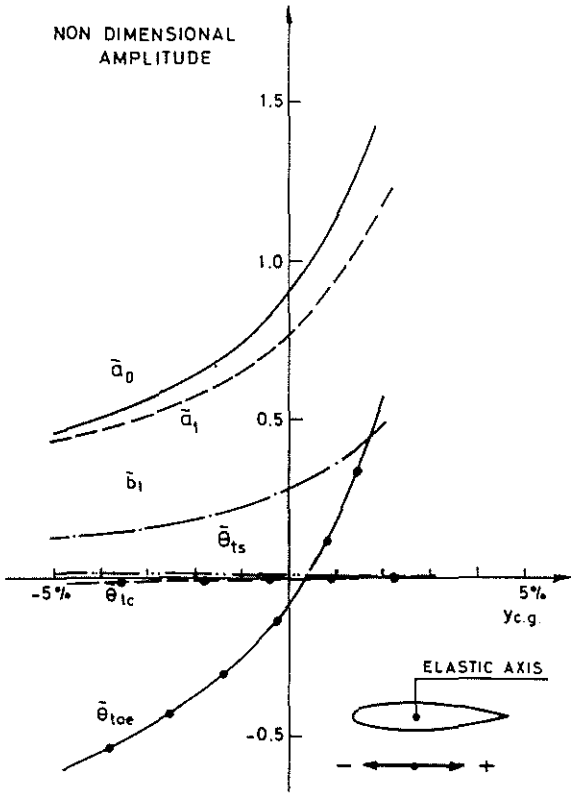

Fig. 4b. The Influence of Cross Sectional Center of Mass Location on the Steady State Flapping and Elastic Pitch in Forward Flight (μ=0.3).

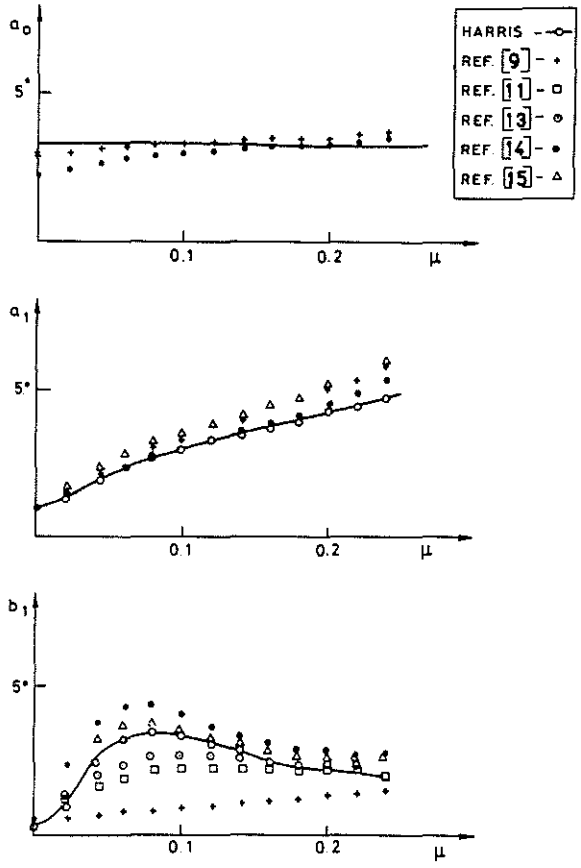

Fig. 5. The Influence of Various Induced Velocity Distributions on the Rotor Flapping - Comparison with the Experimental Results of Harris [17].

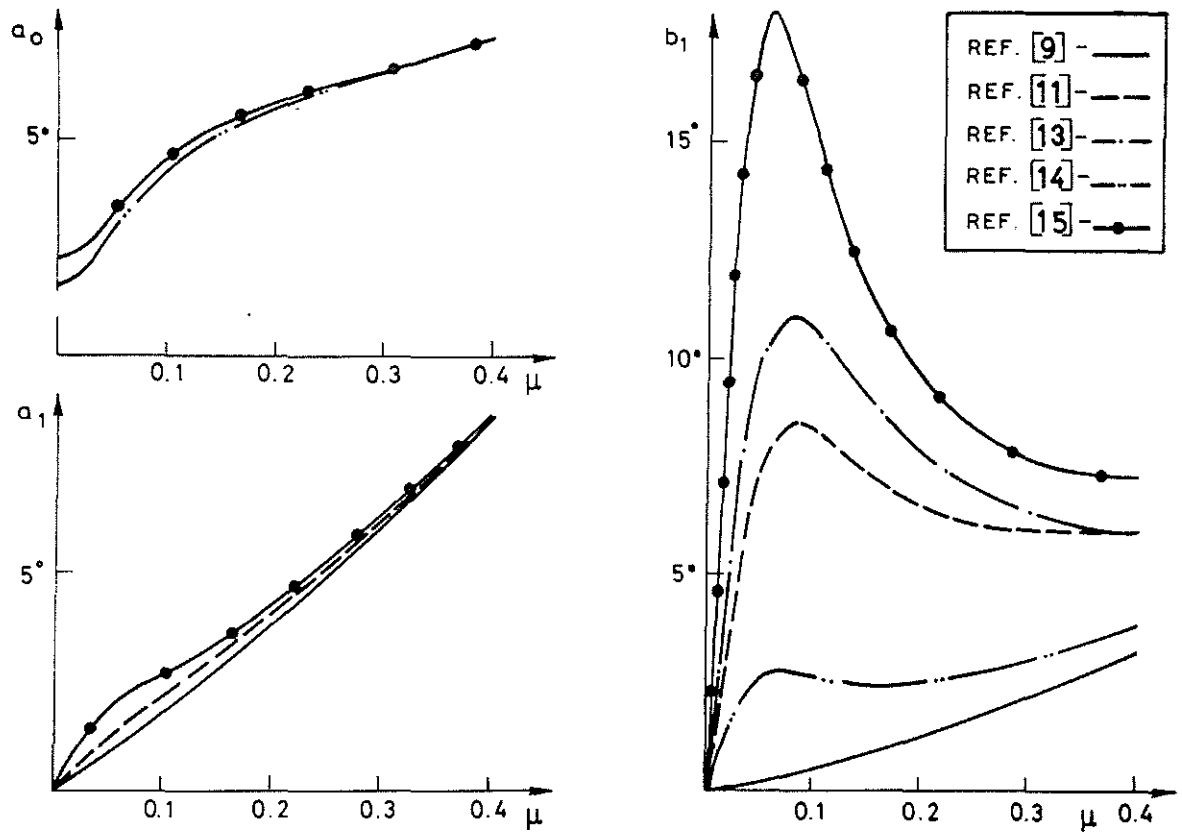

Fig. 6a. The Influence of Various Induced Velocity Distributions on the Rotor Flapping ($y_{ac} = y_{cg} = 0$).

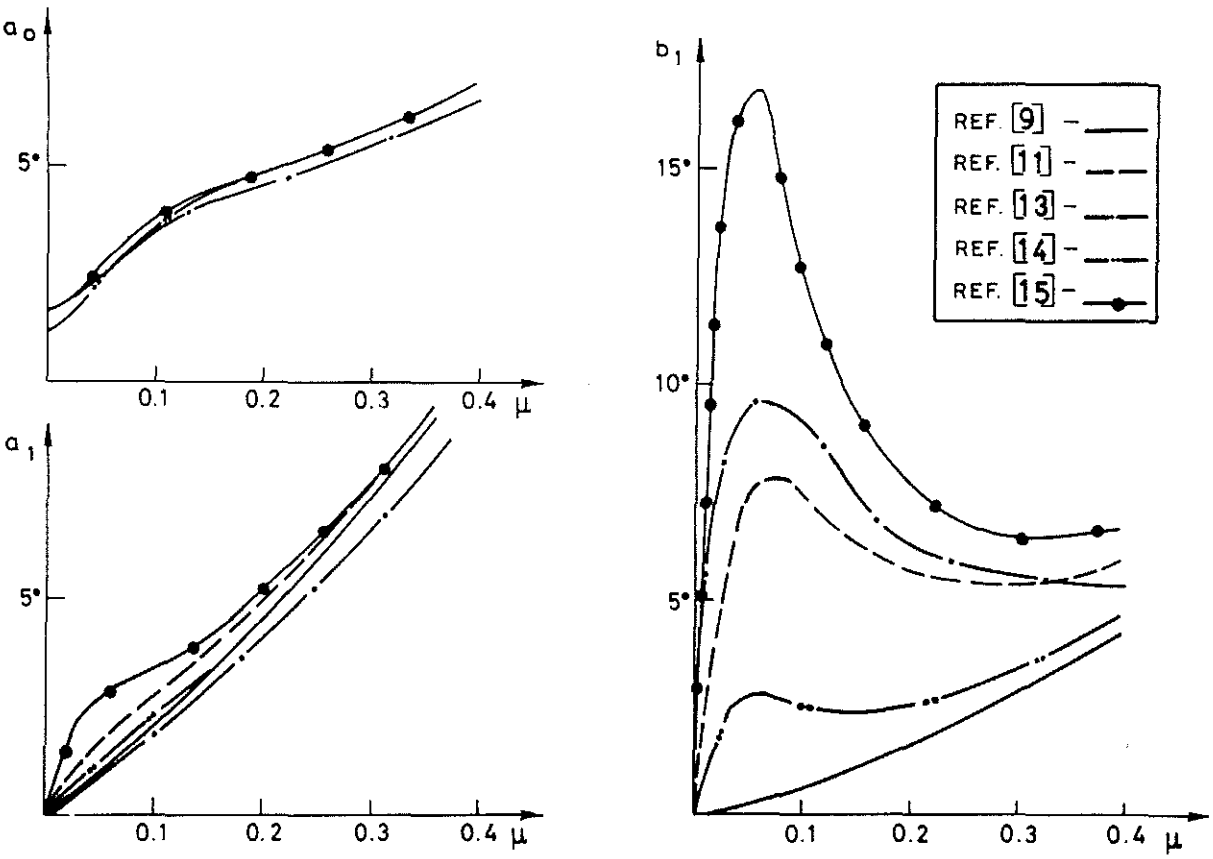

Fig. 6b. The Influence of Various Induced Velocity Distributions on the Rotor Flapping ($y_{ac} = +2\%$; $y_{cg} = 0$).

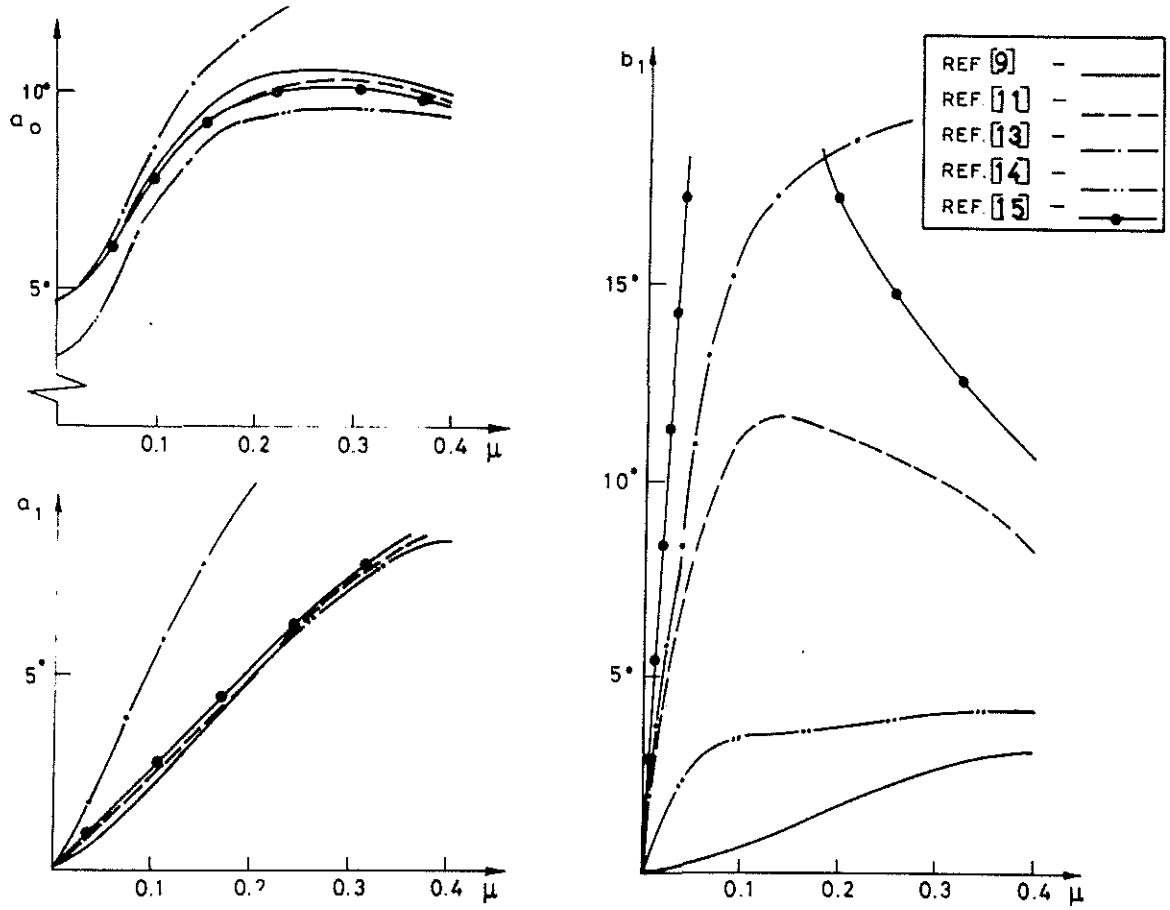

Fig. 6c. The Influence of Various Induced Velocity Distributions on the Rotor Flapping (y_{ac} = -3% ; y_{cg} = 0).

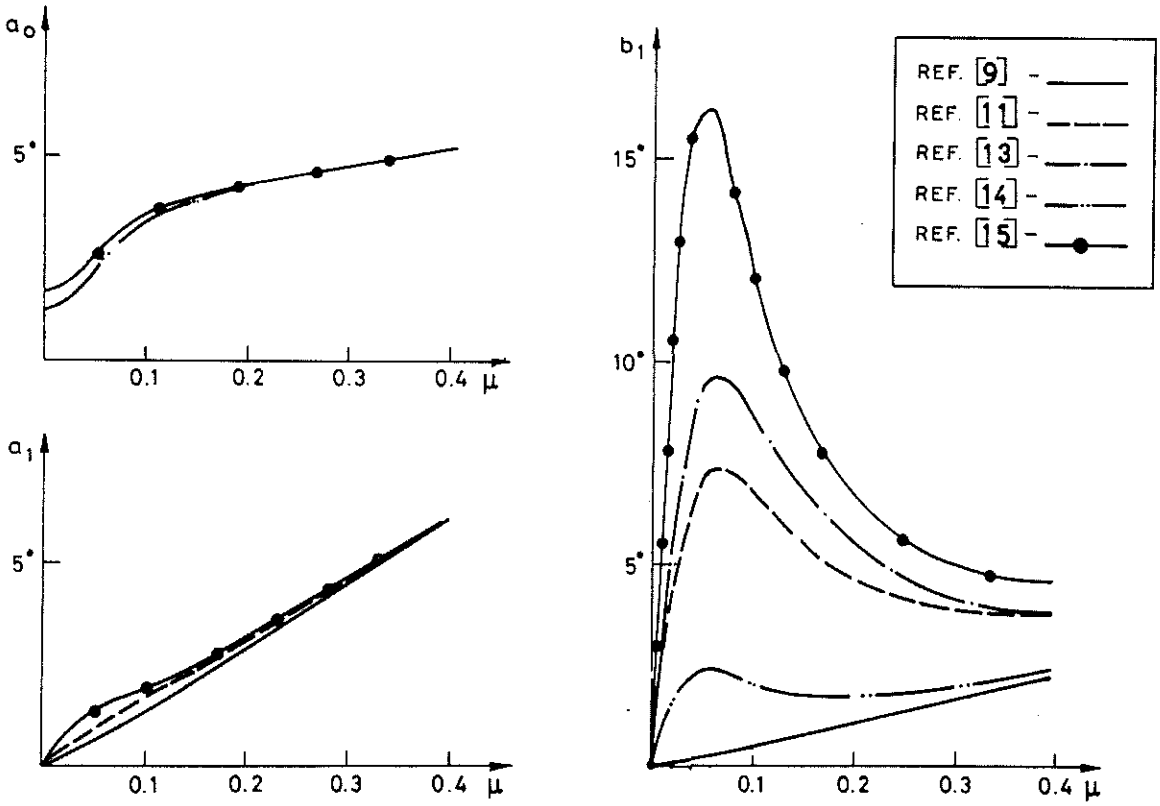

Fig. 6d. The Influence of Various Induced Velocity Distributions on the Rotor Flapping (y_{ac} = 0 ; y_{cg} = -2%).

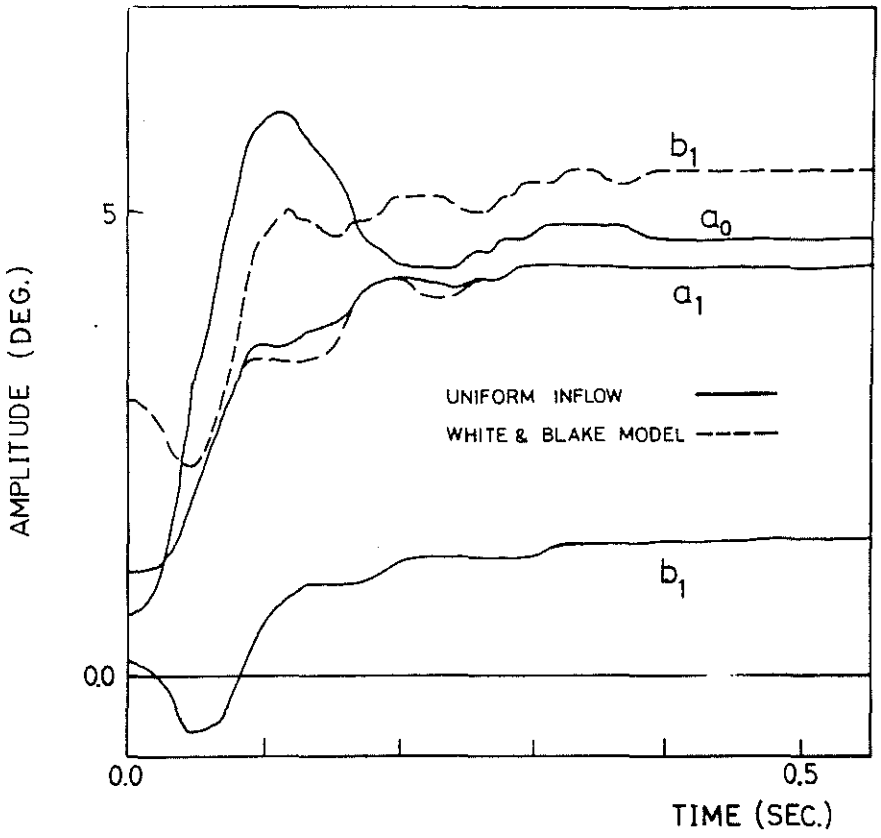

Fig. 7. The Rotor Response to a Step Collective Input-Comparison Between the Uniform and White and Blake Induced Velocity Models (y_{cg} = -2% ; y_{ac} = 0).

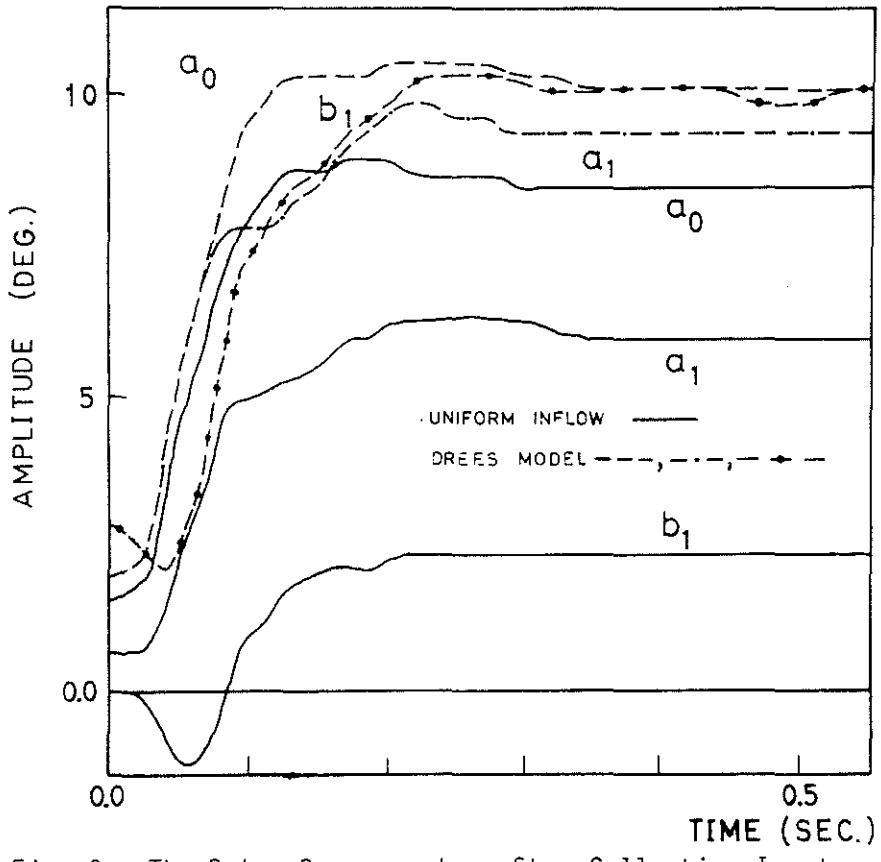

Fig. 8. The Rotor Response to a Step Collective Input-Comparison Between the Uniform and Dress Induced Velocity Models (y_{cg} = 0 ; y_{ac} = -2%).